

Electronic Supplementary Information.

Critical assessment of force fields accuracy against NMR data for cyclic peptides containing β amino acids.

C. Pissoni,^{a†} F. Nardelli,^a S. Zanella,^b F. Curnis,^c L. Belvisi,^b G. Musco^{a} and M. Ghitti^{a*}.*

a Biomolecular NMR Unit, IRCCS Ospedale San Raffaele, Via Olgettina 60, 20132 Milan (Italy).

b Dipartimento di Chimica, Università degli Studi di Milano, Via Golgi 19, 20133 Milan (Italy).

c Tumor biology and vascular targeting Unit, IRCCS Ospedale San Raffaele, Via Olgettina 60,
20132 Milan (Italy).

Table Of Contents

S1. NMR experiments

S2. Supplementary Tables.

S3. Supplementary Figures.

S1. NMR experiments.

All the NMR spectra were recorded on a Bruker Avance-600 spectrometer (Bruker BioSpin) equipped with a triple-resonance TCI cryo-probe with an x, y, z shielded pulsed-field gradient coil. Water proton signal was suppressed with excitation sculpting sequence. For each molecule, ^1H -1D, 1D ^1H -TOCSY (Total Correlation Spectroscopy, $t_{\text{mix}}=60$ ms), ^1H - ^1H -TOCSY ($t_{\text{mix}}=60$ ms) and ^1H - ^1H -ROESY (Rotational nuclear Overhauser Effect Spectroscopy, $t_{\text{mix}}=100$ -600 ms, spin-locking field 2.8 kHz) spectra (**Supplementary Figure S1-S5**) have been recorded at a temperature of 280-285 K. For the cyclic hexapeptides ^1H - ^{13}C HSQC (Heteronuclear Single Quantum Coherence) experiments were also performed for carbon resonances assignment; in addition ^1H - ^{13}C HMBC (Heteronuclear Multiple Bond Correlation) were acquired for c(CGisoDGRG) and c(GCisoDGRG). Peptides at a concentration of 1-10 mM were prepared in 20 mM phosphate buffer, pH 6.5 (90% H_2O , 10% D_2O). Free induction decays were acquired (24-64 scans) over 5000-8000 Hz, into 2k data block for 256-512 incremental values of the evolution time. 2D data were processed with TOPSPIN 3.2 (Bruker BioSpin GmbH, Rheinstetten, Germany) by apodization with 90° shifted sine-bell squared window, and zero-filling in the indirect dimension to 1k points. Peptide assignments and peak lists were generated using CcpNmr version 2.4.¹ The $^3J(\text{HN},\text{H}\alpha)$ and $^3J^{\text{isoD}}(\text{H}\alpha,\text{H}\beta)$ coupling constants were obtained directly from the resolved amide, α or β protons resonances of well digitized mono-dimensional spectra (40k points). When possible, the methylene stereo-specific assignments were derived by comparison of the experimental 3J coupling values and relative ROEs intensities.

S2. Supplementary Tables.

Table S1. List of NMR data used for the force field evaluation, subdivided by type (3J scalar coupling or Chemical Shift, CS) and by molecule.

Peptide	3J -couplings		Chemical Shifts					Total
	$^3J(\text{HN}, \text{H}\alpha)$	$^3J^{\text{isoD}}(\text{H}\alpha, \text{H}\beta)$	CS_{C}	$\text{CS}_{\text{C}\alpha}$	$\text{CS}_{\text{C}\beta}$	$\text{CS}_{\text{H}\alpha}$	CS_{HN}	
CisoDGRC	4	2						6
_{ac} CisoDGRC	6	2						8
c(CGisoDGRG)	6	2	3	3	2	4	3	23
c(GCisoDGRG)	7	2	3	3	1	5	3	24
c(CphgisoDGRG)	8	2		2	1	3	2	18
Total	31	10	6	8	4	12	8	79

Table S2. Experimental ^3J couplings and chemical shifts of CisoDGRC. The data used for the comparison are highlighted in bold. Peak overlap and unresolvable multiplets are indicated with a single and double asterisk, respectively. The experimental error estimated for the ^3J couplings is 0.2 Hz.

Residue	^3J couplings [Hz]		Chemical Shifts [ppm]					
	$^3\text{J}(\text{HN}, \text{H}\alpha)$ [Hz]	$^3\text{J}(\text{H}\alpha, \text{H}\beta)$ [Hz]	CS_{HN}	$\text{CS}_{\text{H}\alpha}$	$\text{CS}_{\text{H}\beta}$	$\text{CS}_{\text{H}\gamma}$	$\text{CS}_{\text{H}\delta}$	$\text{CS}_{\text{H}\epsilon}$
C1		4.6, 9.7		4.15	2.91, 3.15			
isoD2	**	9.6, 4.7	8.84	4.46	2.79, 2.92			
G3	7.1, 5.4		8.27	3.66, 3.92				
R4	6.7	**	8.34	4.16	1.63, 1.69	1.51, 1.51	3.05, 3.05	7.08
C5	7.8	3.6, 8.6	8.61	4.49	2.95, 3.28			

Table S3. Experimental ^3J couplings and chemical shifts of acCisoDGRC. The data used for the comparison are highlighted in bold.

Unresolvable multiplets are indicated with a double asterisk. The experimental error estimated for the ^3J couplings is 0.2 Hz.

Residue	^3J couplings [Hz]		Chemical Shifts [ppm]						
	$^3\text{J}(\text{HN}, \text{H}\alpha)$ [Hz]	$^3\text{J}(\text{H}\alpha, \text{H}\beta)$ [Hz]	CS _{Hac}	CS _{HN}	CS _{Hα}	CS _{Hβ}	CS _{Hγ}	CS _{Hδ}	CS _{Hϵ}
acC1	8.7	2.6, 10.3	2.07	8.37	4.63	2.69, 3.31			
isoD2	8.1	10.0, 3.7		7.88	4.50	2.59, 2.86			
G3	5.4, 6.7			8.16	3.88, 4.03				
R4	5.7	**		8.28	4.27	1.84, 1.84	1.66, 1.66	3.18, 3.18	7.14
C5	7.1	3.3, 10.4		8.24	4.37	2.94, 3.23			

Table S4. Experimental ^3J couplings and chemical shifts of c(CGisoDGRG). The data used for the comparison are highlighted in bold. Peak overlap and unresolvable multiplets are indicated with a single and double asterisk, respectively. The experimental error estimated for the ^3J couplings is 0.2 Hz.

Residue	^3J couplings [Hz]		Chemical Shifts [ppm]										
	$^3\text{J}(\text{HN},\text{H}\alpha)$ [Hz]	$^3\text{J}(\text{H}\alpha,\text{H}\beta)$ [Hz]	CS_{C}	$\text{CS}_{\text{C}\alpha}$	$\text{CS}_{\text{C}\beta}$	$\text{CS}_{\text{C}\gamma}$	$\text{CS}_{\text{C}\delta}$	CS_{HN}	$\text{CS}_{\text{H}\alpha}$	$\text{CS}_{\text{H}\beta}$	$\text{CS}_{\text{H}\gamma}$	$\text{CS}_{\text{H}\delta}$	$\text{CS}_{\text{H}\epsilon}$
C1	8.5	4.4, 7.3	176.76	57.69	28.33			8.18	4.71	2.94, 2.97			
G2	5.0, 6.2		173.62	45.92				8.45	4.12, 3.87				
isoD3	8.6	7.2, 4.0	176.33	54.50	40.52			7.76	4.53	2.75, 2.85			
G4	*		174.80	45.48				8.47	3.91, 3.87				
R5	*	**	177.74	56.83	30.08	27.04	43.32	8.47	4.32	1.89, 1.89	1.63, 1.69	3.22, 3.22	7.25
G6	5.5, 4.6		174.79	45.90				8.94	4.14, 3.88				

Table S5. Experimental 3J couplings and chemical shifts of c(GCisoDGRG). The data used for the comparison are highlighted in bold.

Unresolvable multiplets are indicated with a double asterisk. The experimental error estimated for the 3J couplings is 0.2 Hz.

Residue	3J couplings [Hz]		Chemical Shifts [ppm]										
	$^3J(\text{HN}, \text{H}\alpha)$ [Hz]	$^3J(\text{H}\alpha, \text{H}\beta)$ [Hz]	CS_C	$\text{CS}_{\text{C}\alpha}$	$\text{CS}_{\text{C}\beta}$	$\text{CS}_{\text{C}\gamma}$	$\text{CS}_{\text{C}\delta}$	CS_{HN}	$\text{CS}_{\text{H}\alpha}$	$\text{CS}_{\text{H}\beta}$	$\text{CS}_{\text{H}\gamma}$	$\text{CS}_{\text{H}\delta}$	$\text{CS}_{\text{H}\epsilon}$
G1	5.7, 6.4		174.99	45.89				8.12	3.99, 4.15				
C2	9.1	4.6, 8.4	173.99	57.73	27.97			8.04	4.70	2.84, 2.98			
isoD3	7.5	10.7, 3.6	175.95	54.82	39.98			8.26	4.47	2.78, 2.89			
G4	**		175.15	44.91				8.39	4.21, 3.83				
R5	4.7	**	177.64	57.37	30.18	27.06	43.4	8.59	4.23	1.83, 1.83	1.66, 1.67	3.22, 3.22	7.31
G6	4.5, 4.5		175.47	45.82				8.93	3.95, 4.01				

Table S6. Experimental ^3J couplings and chemical shifts of c(CphgisoDGRG). The data used for the comparison are highlighted in bold.Unresolvable multiplets are indicated with a double asterisk. The experimental error estimated for the ^3J couplings is of 0.2 Hz.

Residue	^3J couplings [Hz]		Chemical Shifts [ppm]									
	$^3\text{J}(\text{HN},\text{H}\alpha)$ [Hz]	$^3\text{J}(\text{H}\alpha,\text{H}\beta)$ [Hz]	$\text{CS}_{\text{C}\alpha}$	$\text{CS}_{\text{C}\beta}$	$\text{CS}_{\text{C}\gamma}$	$\text{CS}_{\text{C}\delta}$	CS_{HN}	$\text{CS}_{\text{H}\alpha}$	$\text{CS}_{\text{H}\beta}$	$\text{CS}_{\text{H}\gamma}$	$\text{CS}_{\text{H}\delta}$	$\text{CS}_{\text{H}\epsilon}$
C1	7.7	4.8, 6.3	57.89	28.17			8.12	4.60	2.91, 3.02			
phg2	7.5		60.60				8.53	5.59		7.49	7.46	
isoD3	7.6	8.6, 3.2	55.13	41.46			7.81	4.57	2.58, 2.85			
G4	5.9, 5.9		45.80				8.44	3.91, 3.91				
R5	7.6	**	55.99	30.99	27.2	43.37	8.43	4.51	2.00, 2.00	1.69, 1.69	3.24, 3.24	7.26
G6	4.8, 4.8		46.40				8.83	3.83, 4.07				

Table S7. RESP atomic partial charges computed for Phenylglycine and isoAspartate. Equivalent atoms are indicated with *.

Phenylglycine		isoAspartate	
Atom names	Partial Charges	Atom names	Partial Charges
N	-0.3515	N	-0.6589
H	0.2453	H	0.3423
C α	-0.0660	C α	0.1271
H α	0.1388	H α	0.0597
C β	-0.0197	C β	-0.0177
C γ *	-0.0729	H β *	0.0031
H γ *	0.1071	C γ	0.7753
C δ *	-0.1717	O γ *	-0.7695
H δ *	0.1455	C	0.4700
CZ	-0.1248	O	-0.5650
HZ	0.1392		
C	0.5367		
O	-0.5140		

Table S8. List of the Collective Variables (CVs) biased during the BE-META calculations for CisoDGRC, _{ac}CisoDGRC and the three cyclic hexapeptides c(XYisoDGRG), where X and Y must be replaced by Gly, Cys or phg. The CVs used in the clustering procedure are highlighted with a star. The three dihedral angles associated to isoAspartate backbone are denoted as $\phi'(C_{i-1}-N_i-C\alpha_i-C\beta_i)$, $\xi(N_i-C\alpha_i-C\beta_i-C_i)$ and $\xi_1(C\alpha_i-C\beta_i-C_i-N_{i+1})$, the dihedral angles involved in the disulfide bridge between Cys *a* and *b* are denoted as $\chi_{1a}(N_a-C\alpha_a-C\beta_a-S_a)$, $\chi_{2a}(C\alpha_a-C\beta_a-S_a-S_b)$ and $\chi_3(C\beta_a-S_a-S_b-C\beta_b)$.

c(XYisoDGRG)	CisoDGRC	_{ac} CisoDGRC
(ϕ, ψ^*)X1	(ψ^*, χ_1, χ_2)C1	($\phi, \psi^*, \chi_1, \chi_2$) _{ac} C1
(ϕ, ψ^*)Y2	(ϕ', ξ^*, ξ_1^*)isoD2	(ϕ', ξ^*, ξ_1^*)isoD2
(ϕ', ξ^*, ξ_1^*)isoD3	(ϕ, ψ^*)G3	(ϕ, ψ^*)G3
(ϕ, ψ^*)G4	(ϕ, ψ^*)R4	(ϕ, ψ^*)R4
(ϕ, ψ^*)R5	(ϕ, χ_1^*, χ_2)C5	(ϕ, χ_1^*, χ_2)C5
(ϕ, ψ^*)G6	(χ_3)C5-C1	(χ_3)C5- _{ac} C1

Table S9. Set of Karplus parameters used for the back-calculation of ${}^3J(\text{HN},\text{H}\alpha)$ and ${}^3J^{\text{isoD}}(\text{H}\alpha,\text{H}\beta)$.

The associated error σ is also reported.

Torsion (θ)	Scalar Coupling	δ [$^\circ$]	SET	A [Hz]	B [Hz]	C [Hz]	σ [Hz]
ϕ	${}^3J(\text{HN},\text{H}\alpha_{2/3})$	-60 / +60	ORIG ²	7.09	-1.42	1.55	0.70
			DFT ³	9.44	-1.53	-0.07	0.70
			Cung et al. ^{4,5}	10.2	-1.8	1.9	1.00
$\xi(\text{N}-\text{C}\alpha-\text{C}\beta-\text{C})$	${}^3J^{\text{isoD}}(\text{H}\alpha,\text{H}\beta_{2/3})$	-120 / ± 0	De Marco et al. ^{6,7}	9.5	-1.6	1.8	1.00
			Perez et al. ⁸	7.23	-1.37	2.40	1.00

Table S10. Estimated errors for the chemical shift predictions, as reported by the Sparta+ developer.⁹

Error [ppm]	Atoms				
	C	C α	C β	HN	H α
	1.09	0.94	1.14	0.49	0.25

Table S11: Comparison between experimental and back-calculated Chemical Shifts. Peptide code was assigned according to Figure 1. Estimated errors for the chemical shift predictions are reported in Table S10.

Peptide	Residue	Experimental CS [ppm]	ff99sb	ff99sb-ildn	ff99sb*	ff14sb	OPLS-AA/L	OPLS-AA/L _{STD}	CHARMM27	GROMOS-54a7	
C1	CS _C	176.76	175.54	175.35	175.54	175.50	175.39	175.27	175.19	175.39	
	CS _{Cα}	57.69	58.81	58.73	58.92	59.21	58.46	58.55	58.61	58.72	
	CS _{Cβ}	28.33	28.01	28.03	28.03	27.62	28.61	28.83	27.87	28.24	
	CS _{HN}	8.18	8.14	8.13	8.18	8.19	8.18	8.16	8.07	8.17	
	CS _{Hα}	4.71	4.53	4.56	4.55	4.45	4.73	4.75	4.59	4.48	
3	R5	CS _C	177.74	176.64	176.79	176.72	176.78	176.64	176.73	176.78	177.21
	CS _{Cα}	56.83	56.09	55.94	56.06	56.18	56.60	56.75	55.94	56.39	
	CS _{Cβ}	30.08	30.39	30.61	30.61	30.46	30.51	30.34	30.76	30.23	
	CS _{HN}	8.47	8.32	8.27	8.28	8.30	8.48	8.53	8.20	8.44	
	CS _{Hα}	4.32	4.35	4.38	4.39	4.33	4.40	4.37	4.38	4.28	
G6	CS _C	174.79	174.65	174.83	174.70	174.68	174.25	174.40	174.65	174.76	
	CS _{Cα}	45.90	45.47	45.73	45.54	45.40	44.80	44.83	45.59	45.60	
	CS _{HN}	8.94	8.49	8.58	8.46	8.47	8.42	8.51	8.63	8.65	
	CS _{Hα}	4.14	3.74	3.71	3.76	3.75	3.81	3.77	3.75	3.67	
			3.88	3.74	3.71	3.76	3.75	3.80	3.77	3.75	3.67
G1	CS _C	174.99	174.67	174.69	174.84	174.68	173.91	173.90	174.97	173.94	
	CS _{Cα}	45.89	45.26	45.21	45.29	45.16	44.80	44.83	44.98	45.03	
	CS _{HN}	8.12	8.26	8.20	8.29	8.13	8.11	8.10	8.13	8.16	
	CS _{Hα}	3.99	3.76	3.75	3.73	3.76	3.97	4.00	3.68	3.83	
			4.15	3.76	3.75	3.73	3.75	3.97	4.00	3.67	3.83
4	R5	CS _C	177.64	176.34	176.49	176.40	176.63	176.50	176.54	176.39	176.98
	CS _{Cα}	57.37	56.15	56.42	56.25	56.58	56.67	56.66	56.65	56.56	
	CS _{Cβ}	30.18	30.40	30.09	30.74	29.98	30.27	30.07	29.36	30.12	
	CS _{HN}	8.59	8.37	8.49	8.35	8.53	8.53	8.57	8.69	8.48	
	CS _{Hα}	4.22	4.31	4.22	4.34	4.19	4.36	4.32	4.07	4.24	
G6	CS _C	175.47	174.74	174.76	174.77	174.67	174.28	174.31	174.77	174.50	
	CS _{Cα}	45.82	45.05	45.06	45.10	44.99	44.69	44.70	44.85	45.05	
	CS _{HN}	8.93	8.43	8.50	8.44	8.46	8.43	8.42	8.54	8.52	
	CS _{Hα}	3.95	3.76	3.73	3.78	3.74	3.84	3.85	3.72	3.73	
			4.01	3.76	3.73	3.78	3.74	3.84	3.85	3.72	3.73
5	R5	CS _{Cα}	55.99	56.01	56.10	56.14	56.38	56.50	56.52	57.33	56.06
	CS _{Cβ}	30.99	30.68	30.62	30.69	30.38	30.82	30.61	30.27	30.42	
	CS _{HN}	8.43	8.29	8.32	8.31	8.38	8.47	8.49	8.63	8.33	
	CS _{Hα}	4.51	4.44	4.36	4.40	4.27	4.50	4.43	4.32	4.42	
	G6	CS _{Cα}	46.40	45.25	45.54	45.48	45.31	44.69	44.78	45.23	45.83
CS _{HN}		8.83	8.40	8.54	8.49	8.46	8.33	8.39	8.51	8.66	
CS _{Hα}		3.83	3.76	3.70	3.73	3.71	3.87	3.79	3.80	3.68	
		4.07	3.77	3.72	3.75	3.73	3.87	3.80	3.83	3.67	

Table S12. Comparison between experimental and back-calculated $^3J(\text{HN},\text{H}\alpha)$. Peptide code was assigned according to Figure 1. The experimental and computational error estimated for the $^3J(\text{HN},\text{H}\alpha)$ couplings is of 0.2 and 0.7 Hz, respectively.

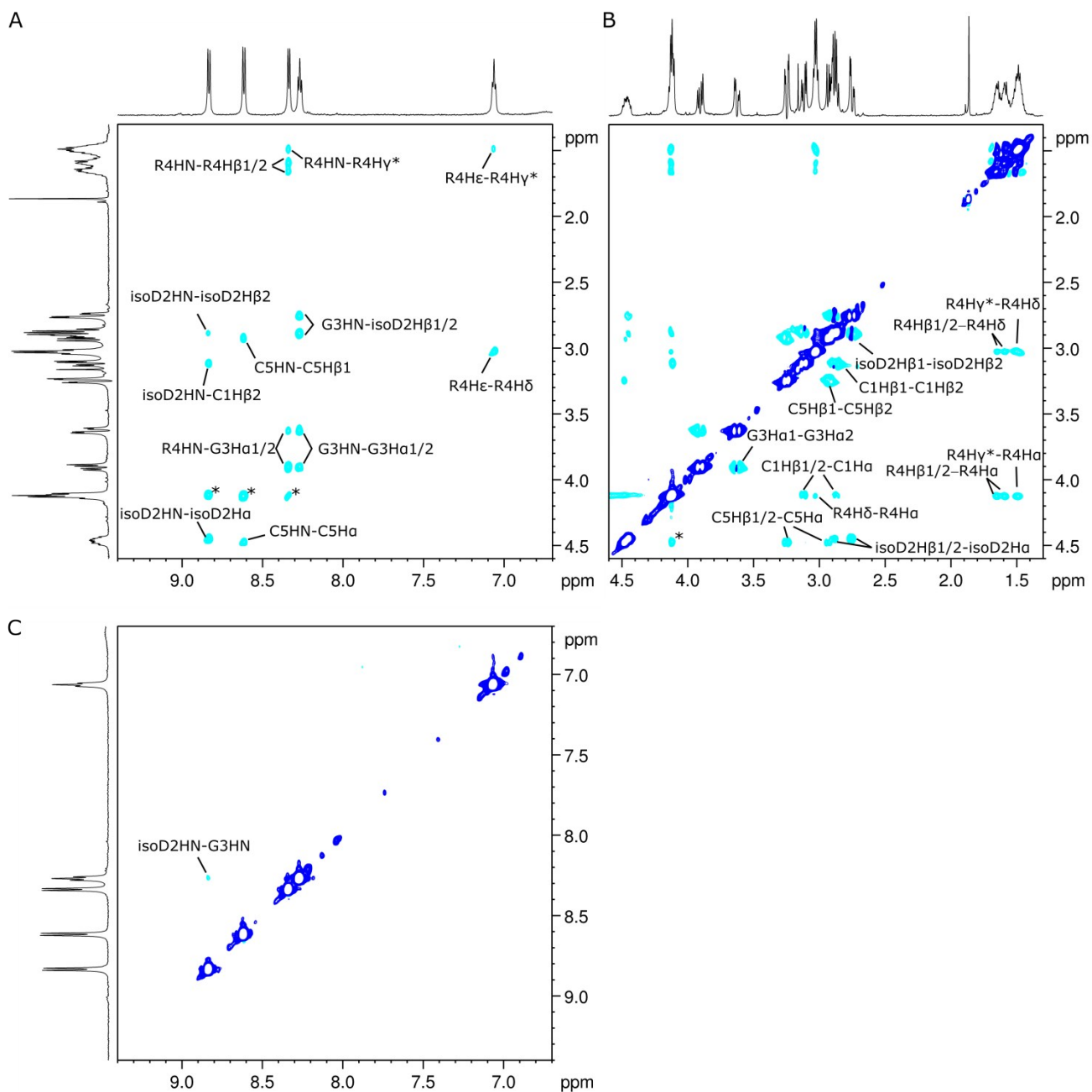
Peptide	Residue	$^3J(\text{HN},\text{H}\alpha)$ [Hz]	ff99sb		ff99sb-ildn		ff99sb*		ff14sb		OPLS-AA/L		OPLS-AA/L _{STD}		CHARMM27		GROMOS-54a7			
			ORIG	DFT	ORIG	DFT	ORIG	DFT	ORIG	DFT	ORIG	DFT	ORIG	DFT	ORIG	DFT	ORIG	DFT	ORIG	DFT
1	G3	7.1	5.9	5.7	5.4	5.1	5.9	5.8	5.4	5.2	4.2	3.5	5.8	5.5	6.1	6.1	5.9	5.9	5.9	5.5
		5.4	6.3	6.2	6.4	6.3	6.1	6.1	6.7	6.7	8.3	8.7	6.8	6.8	6.2	6.0	5.8	5.5	5.5	5.5
	R4	6.7	6.8	6.8	6.8	6.7	6.9	6.9	5.9	5.6	8.5	8.9	7.8	8.0	6.9	7.1	6.0	5.7	5.7	5.7
		C5	7.8	7.7	7.8	7.9	8.1	7.9	8.1	7.0	6.9	7.6	7.7	7.5	7.6	8.3	8.6	7.5	7.5	7.5
2	acC1	8.7	7.7	7.8	7.8	8.0	7.6	7.8	7.1	7.1	7.3	7.3	7.9	8.1	7.9	8.1	6.3	6.1	6.1	6.1
	isoD2	8.1	7.8	8.0	8.1	8.4	7.9	8.1	7.3	7.3	6.7	6.5	6.8	6.6	8.5	8.8	7.2	7.2	7.2	7.2
	G3	5.4	5.9	5.7	5.3	5.0	5.8	5.7	5.4	5.2	4.4	3.8	5.9	5.7	6.1	6.0	5.1	4.8	4.8	4.8
		6.7	5.8	5.6	5.9	5.6	5.8	5.5	6.4	6.1	8.1	8.4	6.4	6.3	6.1	5.9	6.0	5.7	5.7	5.7
	R4	5.7	7.1	7.1	7.2	7.3	7.3	7.3	6.4	6.2	8.4	8.8	7.8	8.0	6.8	6.8	6.4	6.2	6.2	6.2
C5	7.1	7.7	7.9	7.6	7.7	7.7	7.9	6.7	6.6	7.6	7.8	7.7	7.9	8.0	8.2	7.3	7.3	7.3	7.3	
3	C1	8.5	7.5	7.7	7.5	7.6	7.4	7.5	6.5	6.4	7.5	7.5	7.7	7.8	8.0	8.4	5.9	5.6	5.6	5.6
	G2	5.0	5.5	5.3	5.0	4.6	5.5	5.2	5.3	5.0	5.4	5.1	4.6	4.0	5.4	5.2	4.7	4.2	4.2	4.2
		6.2	6.4	6.3	6.7	6.7	6.2	6.0	6.5	6.4	7.2	7.3	8.0	8.4	7.4	7.5	6.1	5.9	5.9	5.9
	isoD3	8.6	7.7	7.9	8.0	8.3	7.9	8.1	6.9	6.9	6.5	6.3	6.5	6.3	8.2	8.5	7.7	7.8	7.8	7.8
	G6	5.5	5.8	5.7	5.8	5.8	5.8	5.7	5.8	5.7	4.5	4.0	4.1	3.5	5.6	5.4	6.2	6.3	6.3	6.3
4.6		5.8	5.6	5.7	5.5	5.8	5.5	5.7	5.4	8.1	8.5	8.5	9.0	6.7	6.9	5.5	5.1	5.1	5.1	
4	G1	5.7	5.9	5.8	5.8	5.7	6.0	6.1	5.8	5.8	6.6	6.6	7.0	7.0	5.8	5.8	5.4	5.1	5.1	5.1
		6.4	6.0	5.7	6.0	5.7	6.0	5.7	6.0	5.7	5.8	5.6	5.5	5.1	7.2	7.2	5.3	4.8	4.8	4.8
	C2	9.1	8.0	8.3	8.1	8.4	8.0	8.3	7.2	7.2	6.7	6.6	7.2	7.2	8.6	9.1	6.1	5.8	5.8	5.8
	isoD3	7.5	7.6	7.8	7.9	8.1	7.6	7.7	7.0	7.0	6.6	6.4	6.5	6.3	7.9	8.1	7.5	7.5	7.5	7.5
	R5	4.7	7.0	7.1	6.4	6.3	6.9	6.9	5.8	5.6	7.3	7.3	7.0	7.1	6.1	6.1	5.6	5.1	5.1	5.1
		4.5	5.8	5.6	6.0	6.0	5.8	5.6	6.2	6.2	4.2	3.5	4.6	4.1	6.0	6.1	6.3	6.4	6.4	6.4
G6	4.5	6.0	5.8	6.1	5.8	6.0	5.8	5.9	5.6	8.5	8.9	8.0	8.3	7.1	7.1	5.3	4.8	4.8	4.8	
5	C1	7.7	7.1	7.1	7.3	7.3	7.3	7.3	6.7	6.5	6.8	6.7	7.0	7.0	8.1	8.4	5.4	4.9	4.9	4.9
	phg2	7.5	7.0	6.9	7.2	7.2	7.1	7.0	7.2	7.2	7.4	7.4	7.8	8.0	7.6	7.7	6.5	6.3	6.3	6.3
	isoD3	7.6	7.6	7.8	7.7	8.0	7.7	7.9	7.0	7.1	6.9	6.8	6.8	6.7	8.5	8.9	7.6	7.7	7.7	7.7
	G4	5.9	6.0	6.0	6.1	6.0	6.1	6.2	5.8	5.7	4.6	4.1	6.4	6.4	5.9	5.9	5.9	5.9	5.9	5.9
		5.9	5.8	5.6	5.5	5.1	5.8	5.6	5.8	5.5	7.9	8.1	6.0	5.8	6.0	5.8	5.6	5.1	5.1	5.1
	R5	7.6	7.6	7.8	7.3	7.4	7.4	7.5	6.4	6.2	7.8	8.0	7.2	7.2	5.7	5.3	6.4	6.2	6.2	6.2
	G6	4.8	5.9	5.8	6.1	6.1	6.0	5.9	6.3	6.3	5.1	4.6	4.4	3.8	6.6	6.6	6.1	6.2	6.2	6.2
4.8		5.7	5.4	5.6	5.2	5.6	5.3	5.5	5.2	7.5	7.6	8.3	8.7	5.8	5.7	5.1	4.6	4.6	4.6	

Table S13. Comparison between experimental and back-calculated $^3J^{\text{isoD}}(\text{H}\alpha, \text{H}\beta)$. Peptide code was assigned according to Figure 1. The experimental and computational error estimated for the $^3J^{\text{isoD}}(\text{H}\alpha, \text{H}\beta)$ couplings is of 0.2 and 1.0 Hz, respectively.

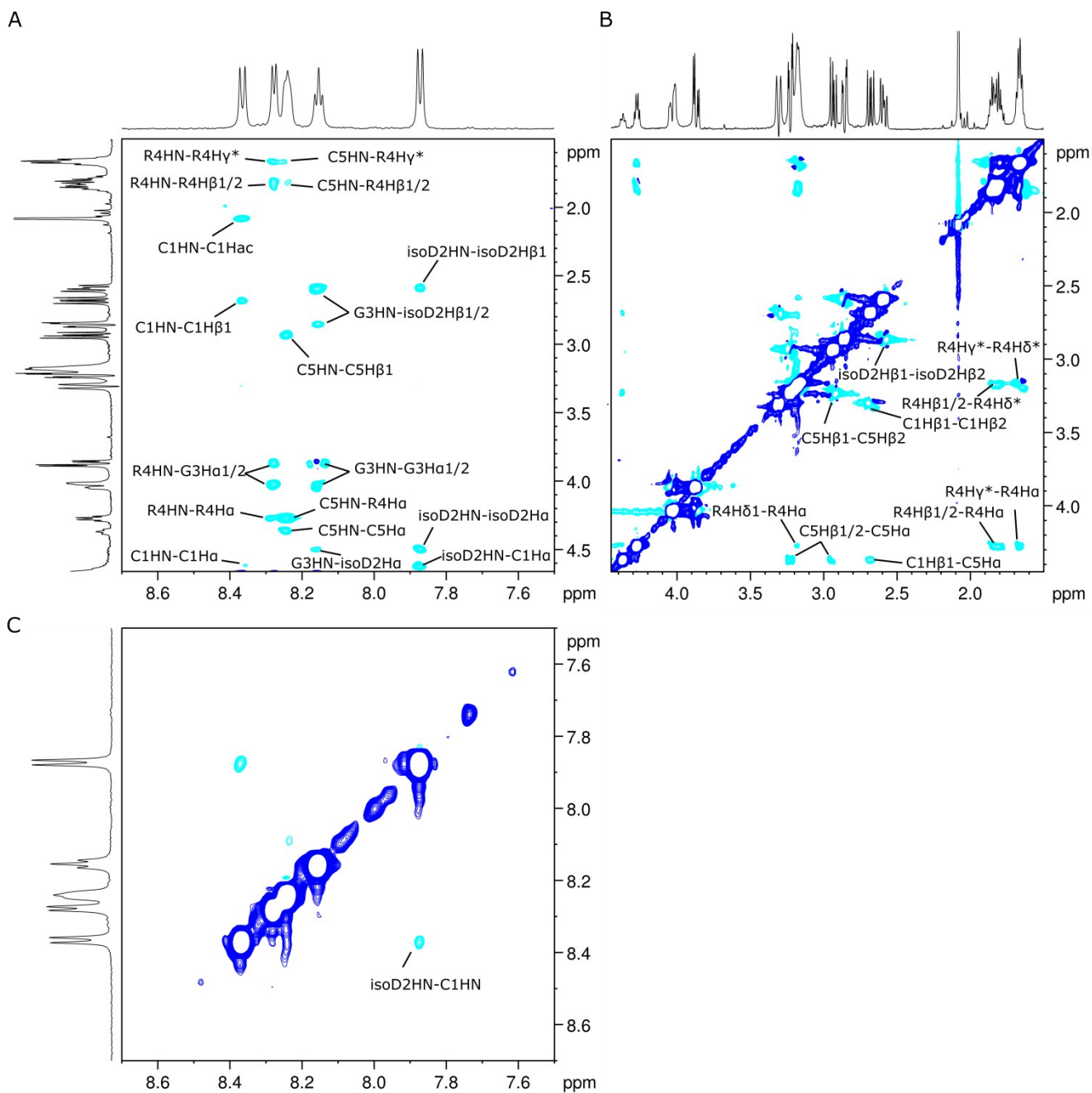
Peptide	$^3J^{\text{isoD}}(\text{H}\alpha, \text{H}\beta)$ [Hz]	ff99sb			ff99sb-ildn			ff99sb*			ff14sb			OPLS-AA/L			OPLS-AA/L _{STD}			CHARMM27			GROMOS-54a7		
		Cung	De Marco	Perez	Cung	De Marco	Perez	Cung	De Marco	Perez	Cung	De Marco	Perez	Cung	De Marco	Perez	Cung	De Marco	Perez	Cung	De Marco	Perez	Cung	De Marco	Perez
1	9.6	7.4	6.9	6.3	12.2	11.3	9.8	8.0	7.5	6.8	12.9	12.0	10.3	2.8	2.7	3.0	3.9	3.6	3.8	12.2	11.3	9.8	6.2	5.8	5.4
	4.7	4.6	4.3	4.3	3.8	3.6	3.7	3.8	3.6	3.7	3.9	3.7	3.7	12.5	11.6	10.0	8.3	7.7	7.0	3.6	3.4	3.6	4.3	4.0	4.0
2	10.0	8.9	8.3	7.4	13.0	12.1	10.4	9.5	8.8	7.8	12.8	11.9	10.2	3.1	3.0	3.2	5.2	4.9	4.7	12.9	12.0	10.3	9.0	8.4	7.5
	3.7	3.6	3.4	3.5	3.4	3.2	3.4	3.5	3.3	3.5	3.6	3.5	3.6	11.5	10.7	9.3	5.3	4.9	4.8	3.5	3.3	3.5	3.8	3.6	3.7
3	7.2	8.8	8.2	7.3	12.9	12.0	10.3	9.4	8.8	7.8	12.4	11.6	10.0	4.6	4.3	4.3	5.4	5.1	4.9	12.2	11.3	9.8	10.7	9.9	8.7
	4.0	3.2	3.0	3.3	3.3	3.1	3.3	3.2	3.1	3.3	3.4	3.3	3.5	5.4	5.1	4.9	4.1	3.9	3.9	3.3	3.1	3.3	3.2	3.1	3.3
4	10.7	7.9	7.4	6.7	11.6	10.8	9.3	6.9	6.4	5.9	11.9	11.0	9.5	5.0	4.7	4.5	4.8	4.6	4.5	12.0	11.2	9.6	10.5	9.8	8.6
	3.6	3.9	3.7	3.8	3.6	3.4	3.6	3.9	3.7	3.8	3.6	3.4	3.6	4.3	4.0	4.1	3.7	3.5	3.6	4.2	3.9	3.9	2.9	2.8	3.1
5	8.6	9.2	8.6	7.6	12.3	11.4	9.8	8.7	8.1	7.2	11.9	11.0	9.5	4.5	4.3	4.3	6.7	6.2	5.8	8.6	8.0	7.2	12.0	11.1	9.6
	3.2	4.0	3.8	3.9	3.6	3.4	3.6	3.5	3.4	3.5	3.7	3.5	3.6	7.9	7.4	6.7	3.9	3.7	3.8	4.5	4.3	4.2	2.9	2.8	3.1

S3. Supplementay Figures

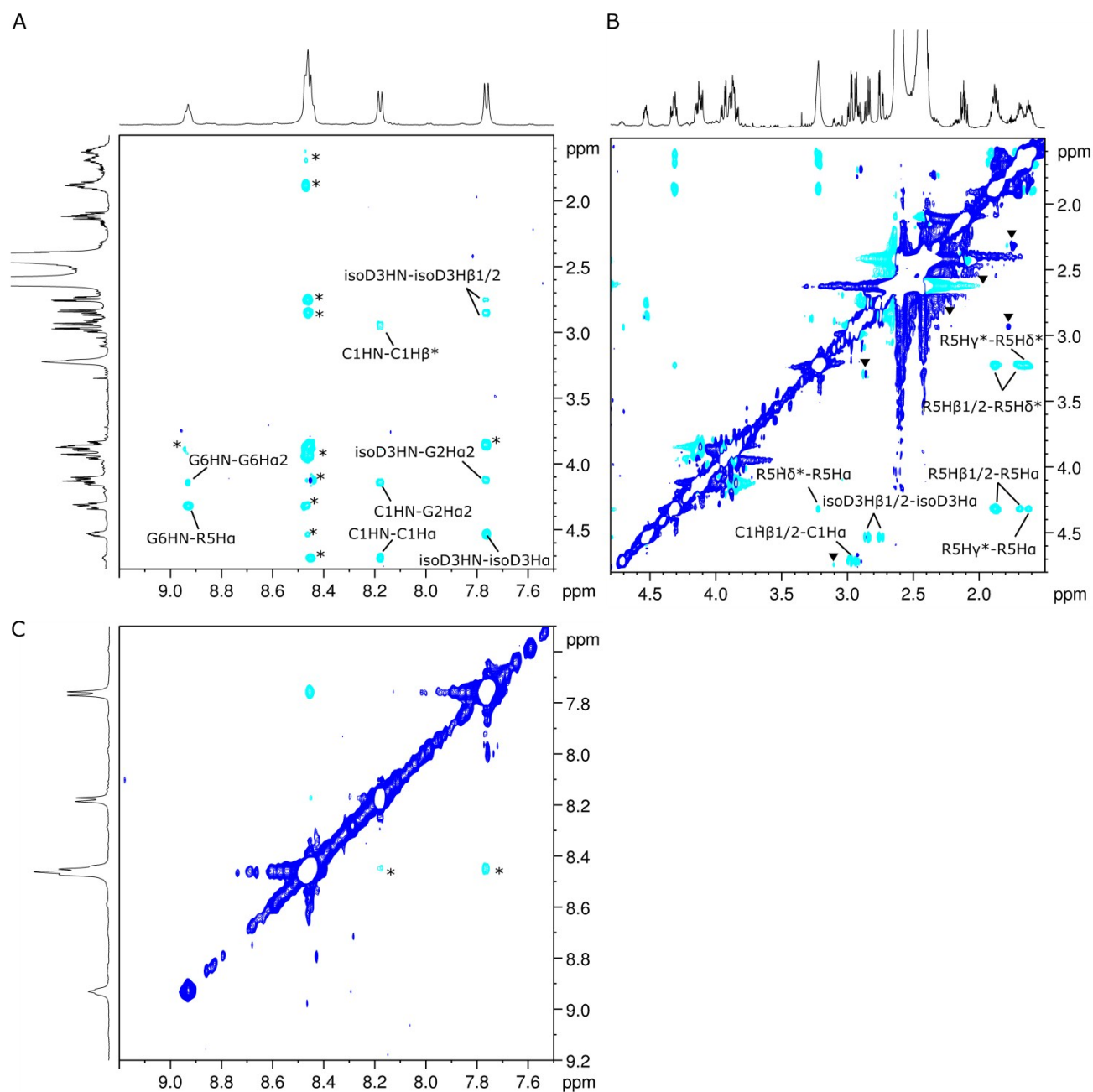
FigS1. ROESY spectrum of CisoDGRC. Expansion of: A) the amide-aliphatic, B) aliphatic-aliphatic and C) amide-amide correlation regions of the ROESY spectrum is reported. Negative peaks (diagonal) are represented in blue, positive cross-peaks are represented in cyan. Overlapping peaks are indicated with an asterisk. The ROESY spectrum was recorded using $t_{\text{mix}} = 0.3$ s.



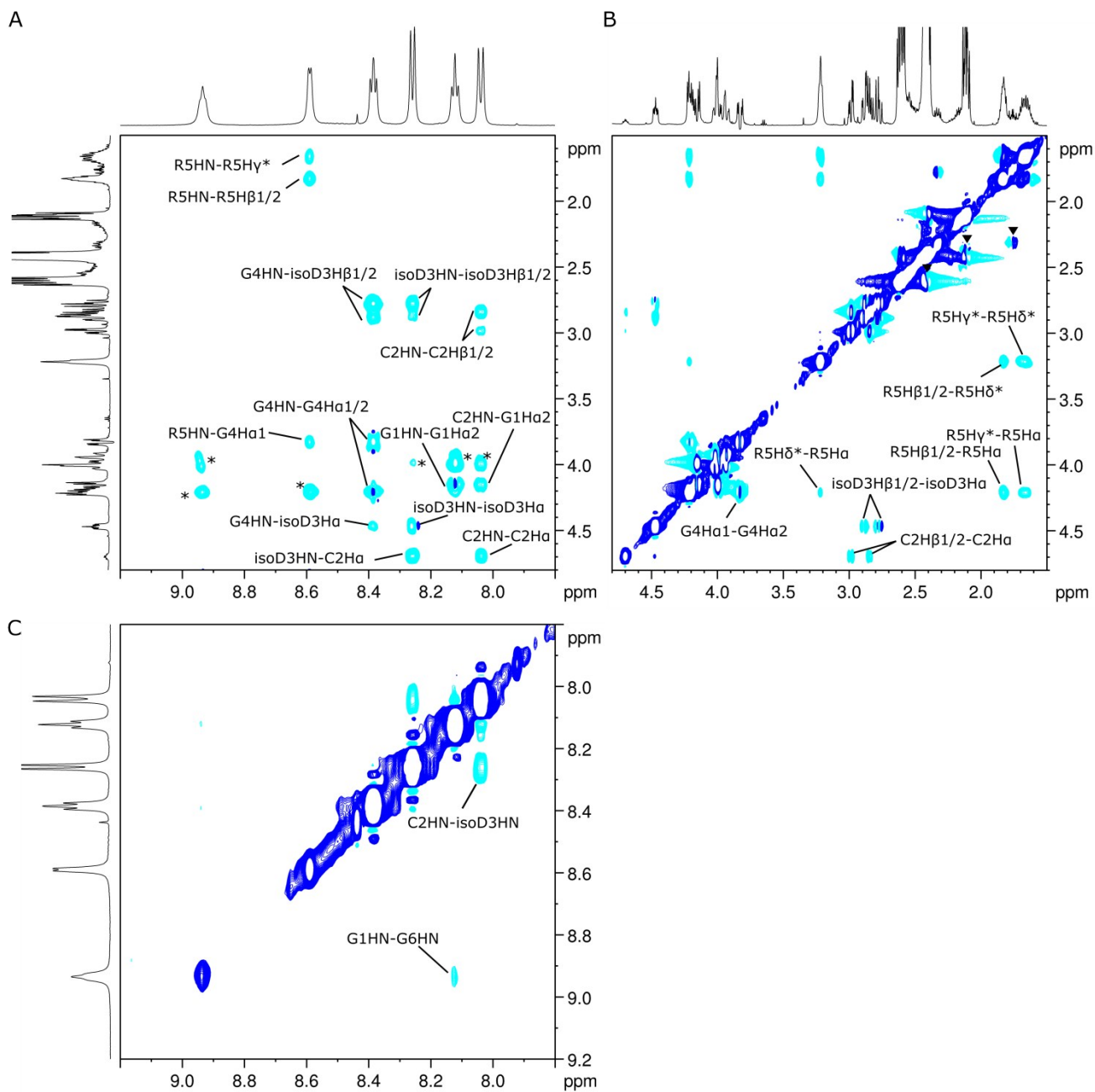
FigS2. ROESY spectrum of acCisoDGRC. Expansion of: A) the amide-aliphatic, B) aliphatic-aliphatic and C) amide-amide correlation regions of the ROESY spectrum is reported. Negative peaks (diagonal) are represented in blue, positive cross-peaks are represented in cyan. Overlapping peaks are indicated with an asterisk. The ROESY spectrum was recorded using $t_{\text{mix}} = 0.3$ s.



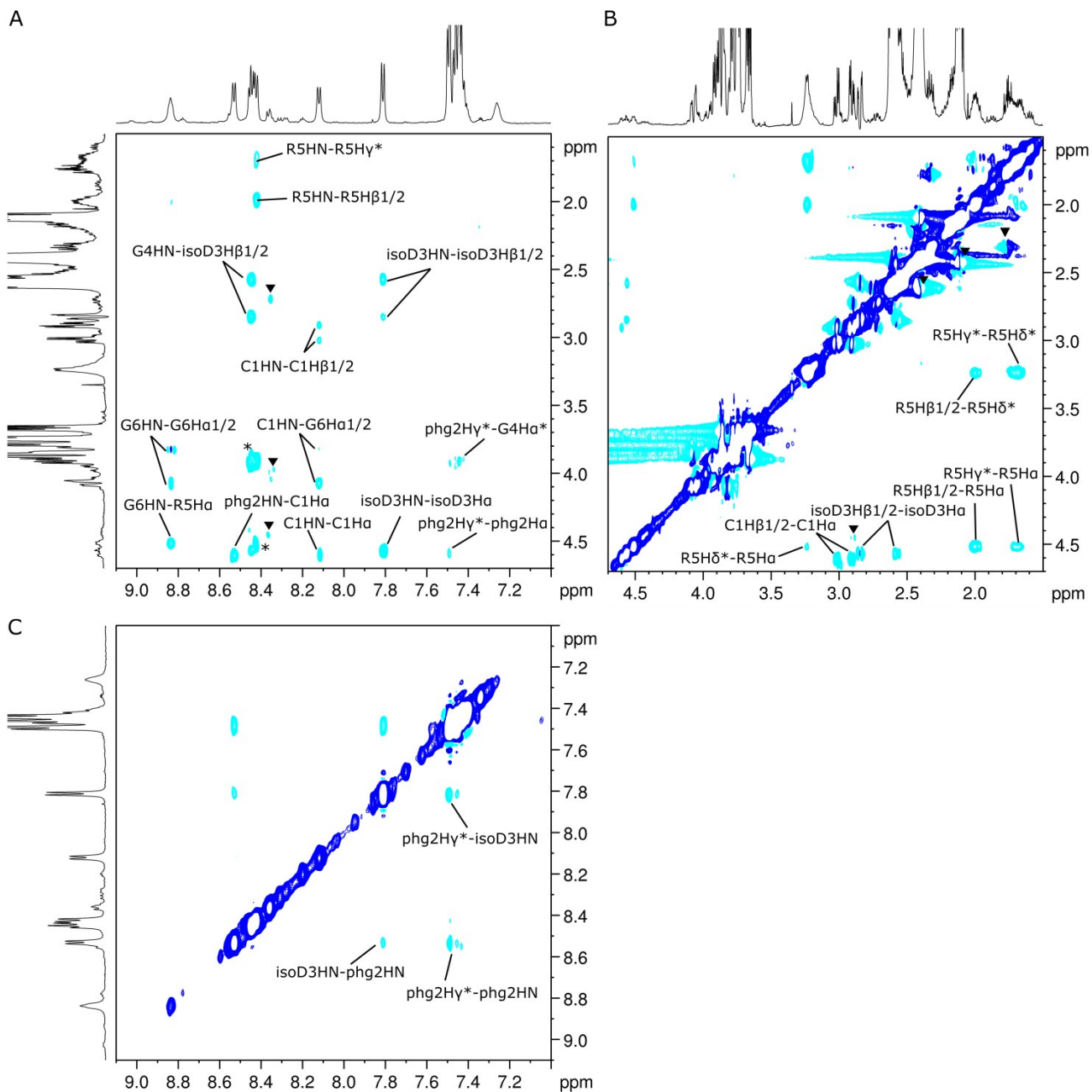
FigS3. ROESY spectrum of c(CGisoDGRG). Expansion of: A) the amide-aliphatic, B) aliphatic-aliphatic and C) amide-amide correlation regions is reported. Negative peaks (diagonal) are represented in blue, positive cross-peaks are represented in cyan. Overlapping peaks and impurities are indicated with an asterisk and a triangle, respectively. The ROESY spectrum was recorded using $t_{\text{mix}} = 0.3$ s.



FigS4. ROESY spectrum of c(GCisoDGRG). Expansion of: A) the amide-aliphatic, B) aliphatic-aliphatic and C) amide-amide correlation regions is reported. Negative peaks (diagonal) are represented in blue, positive cross-peaks are represented in cyan. Overlapping peaks and impurities are indicated with an asterisk and a triangle, respectively. The ROESY spectrum was recorded using $t_{\text{mix}} = 0.3$ s.



FigS5. ROESY spectrum of c(CphgisoDGRG). Expansion of: A) the amide-aliphatic, B) aliphatic-aliphatic and C) amide-amide correlation regions is reported. Negative peaks (diagonal) are represented in blue, positive cross-peaks are represented in cyan. Overlapping peaks and impurities are indicated with an asterisk and a triangle, respectively. The ROESY spectrum was recorded using $t_{\text{mix}} = 0.3$ s.



FigS6. Schematic representation of C-terminal Asparagine (left) and isoAspartic acid (right). The ζ (N-C α -C β -C) dihedral angle characteristic of isoAspartate backbone is highlighted in orange.

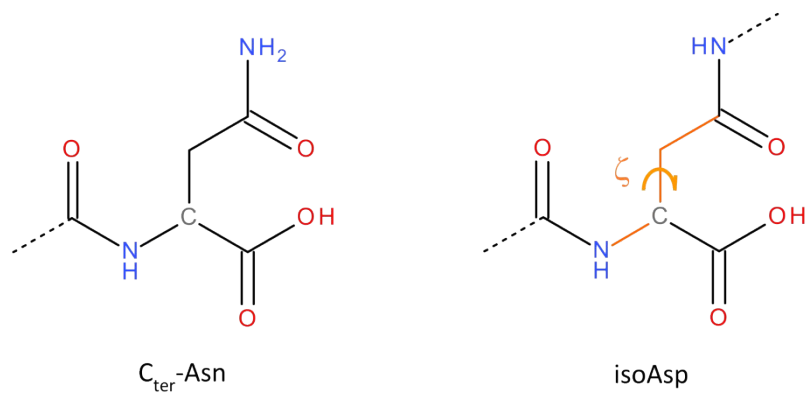


Figure S7. For each force field, the ability to reproduce the experimental chemical shifts is quantified through the χ^2 function.

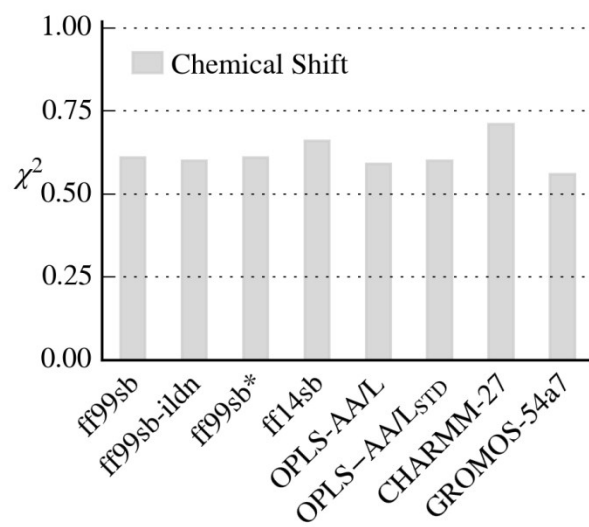


Figure S8. χ^2 values, estimating the ability of each force field to reproduce experimental $^3J(\text{HN},\text{H}\alpha)$ scalar couplings, computed with both the ORIG (light gray bars) and the DFT (blue bars) sets of Karplus parameters. The average χ^2 values and the error bars, representing the standard errors, have been computed adopting a Jack-Knife approach, in which the experimental data associated to one specific molecule have been sequentially excluded as described in Material and Methods.

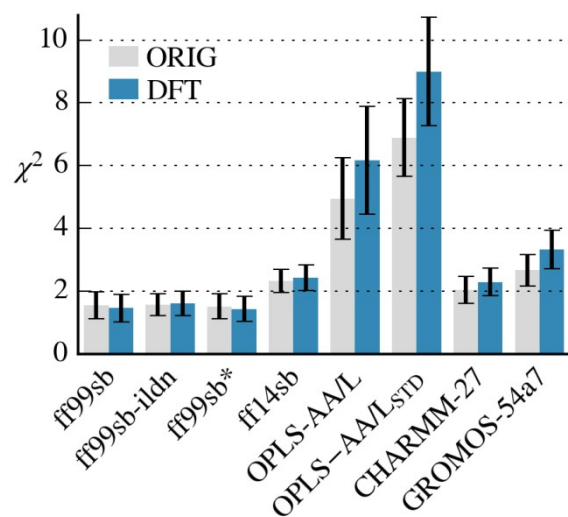


Figure S9. For each force field, the ability to reproduce the experimental $^3J(\text{HN},\text{H}\alpha)$ scalar couplings, considering all the $^3J(\text{HN},\text{H}\alpha)$ couplings (light gray bars) or excluding the $^3J(\text{HN},\text{H}\alpha)$ couplings of isoAspartate residue ($^3J(\text{HN},\text{H}\alpha)^*$, blue bars), is quantified through the χ^2 function. Both the ORIG (upper panel) and the DFT (lower panel) sets of Karplus parameters have been used. The error bars represent the standard deviation of the χ^2 values obtained analyzing separately the first and second halves of each simulation, as described in Material and Methods.

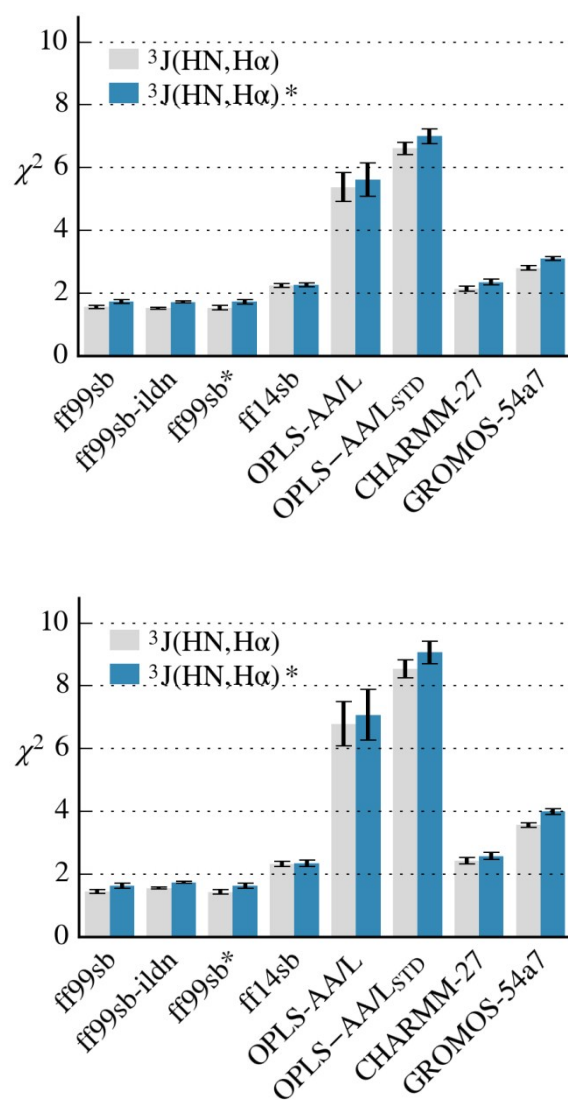


Figure S10. Experimental vs Back-calculated $^3J(\text{HN},\text{H}\alpha)$ calculated using the ORIG (upper panel) and DFT (lower panel) set of Karplus parameters. The grey shadow indicates a deviation of ± 0.7 Hz from experimental data. The r^2 value for linear regression of each force field is also reported.

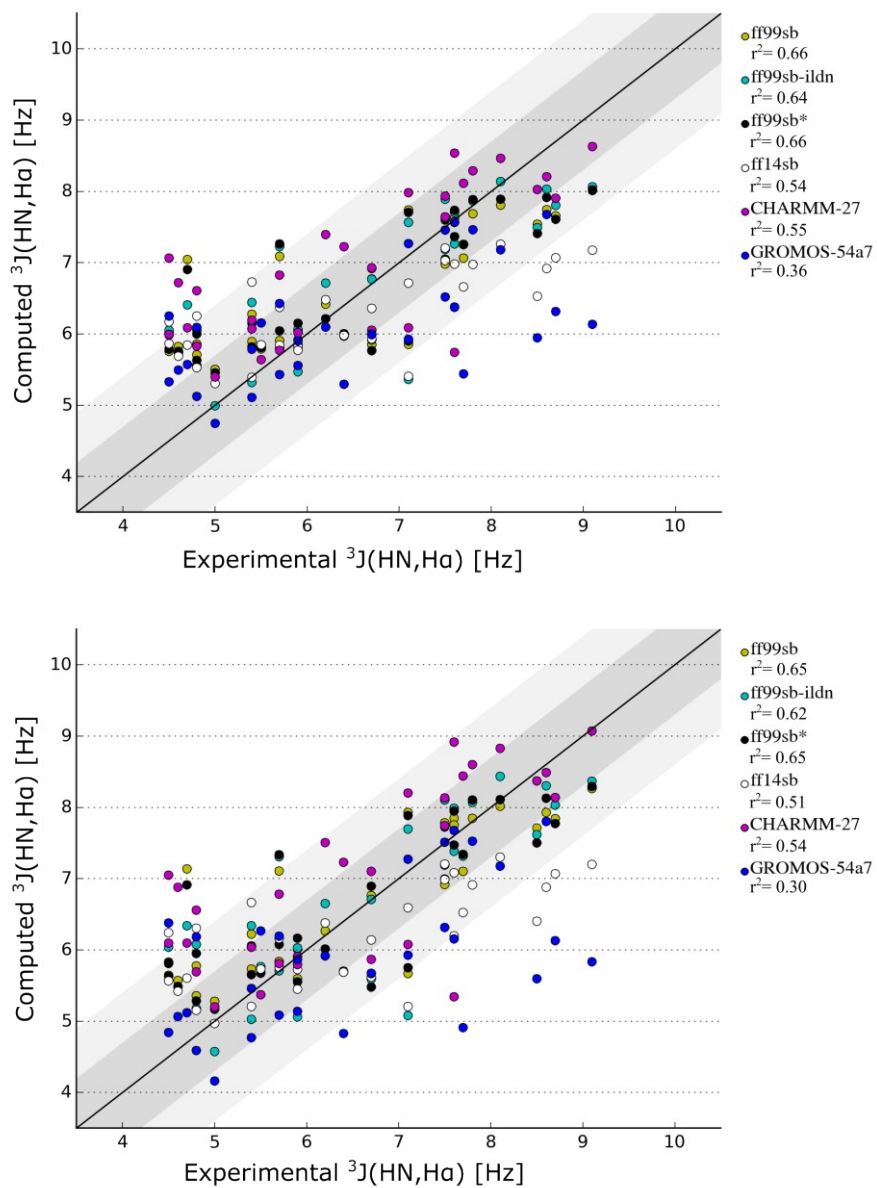
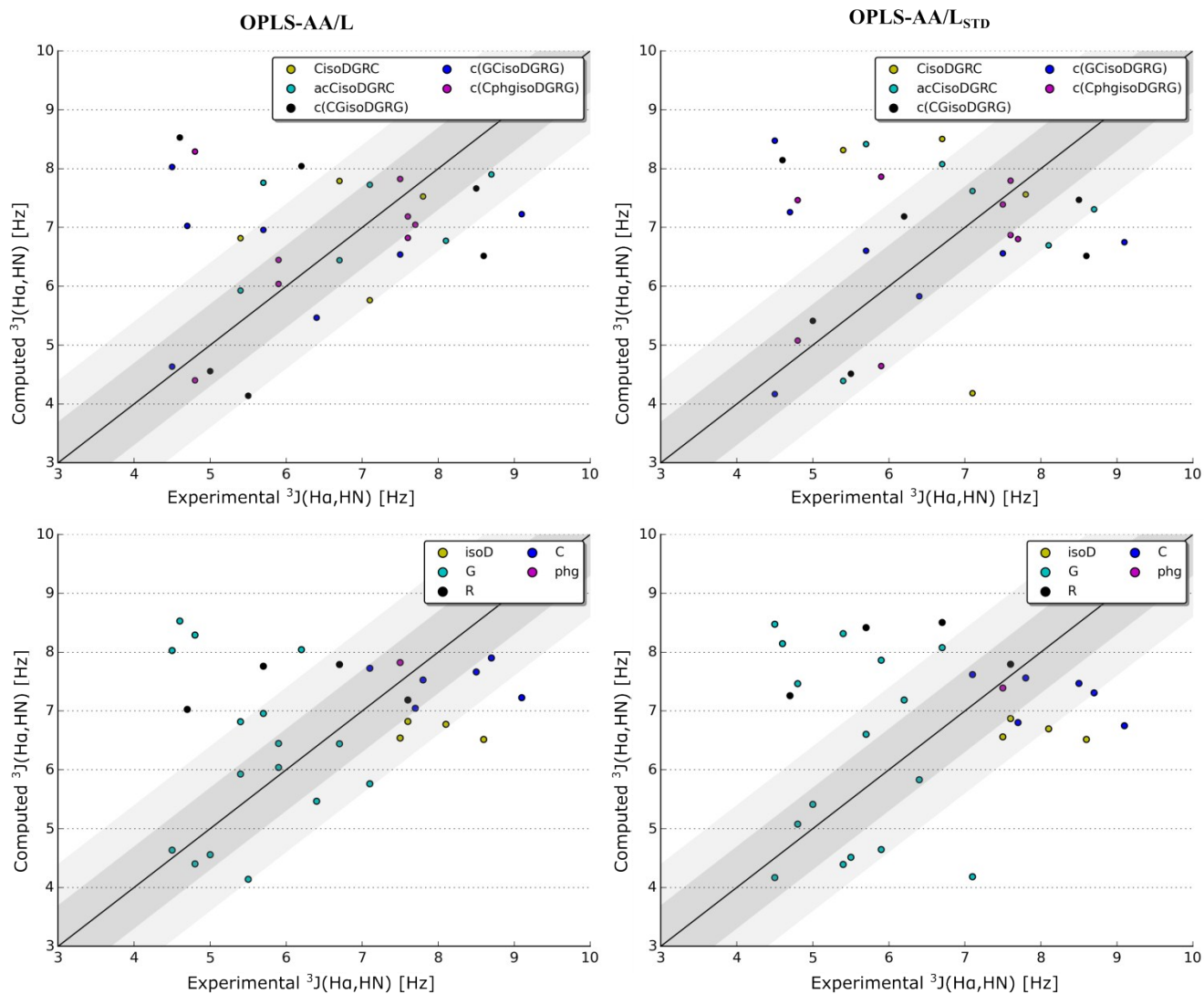


Figure S11. For OPLS force fields, the comparison between experimental and computational $^3J(\text{HN}, \text{H}\alpha)$ of single CP and amino acid, computed with ORIG and DFT parameters is reported in the first and second panel, respectively. The grey shadow indicates a deviation of ± 0.7 Hz from experimental data.



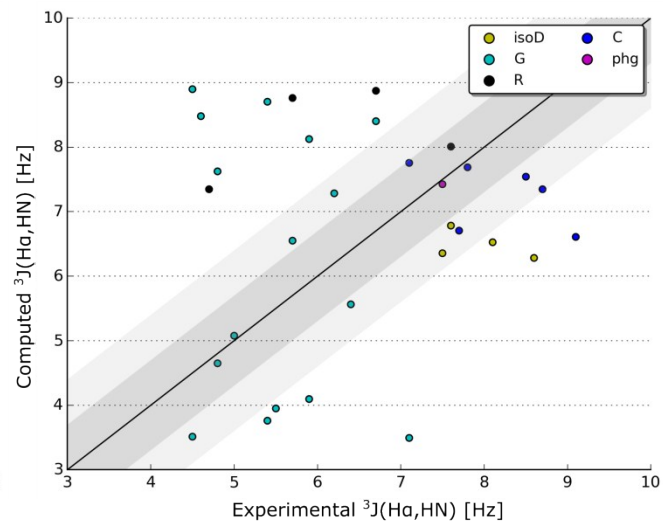
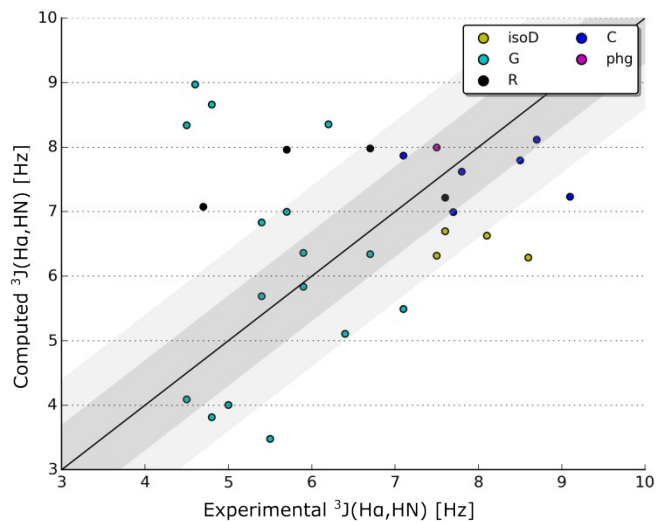
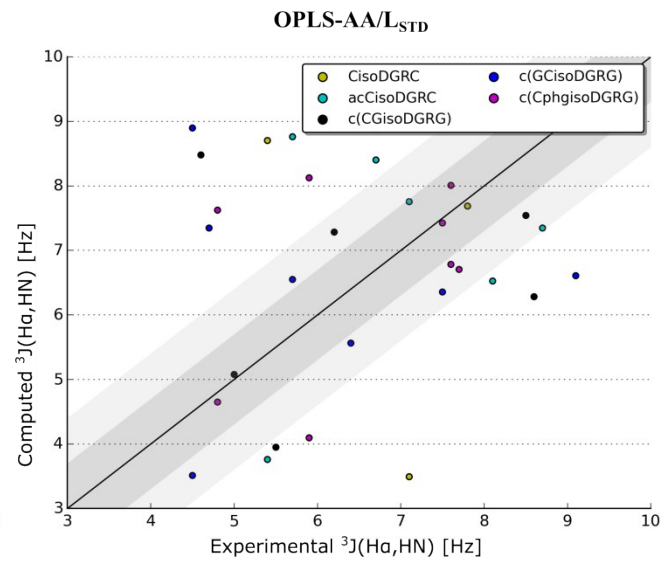
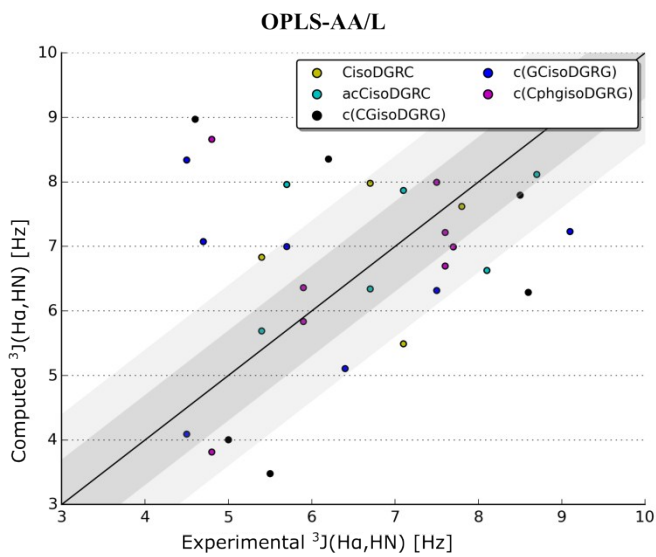


Figure S12. In the upper panel, representation of the Karplus relations for the ${}^3J(\text{H}\alpha, \text{H}\beta)$ scalar coupling as a function of the $\xi(\text{N}-\text{C}\alpha-\text{C}\beta-\text{C})$ dihedral angle, according to the parametrization of Cung et al. (gray), De Marco et al. (blue) and Perez et al. (orange). The offset $\delta=-120^\circ$ has been applied for the ${}^3J^{\text{isoD}}(\text{H}\alpha, \text{H}\beta_2)$ couplings. In the lower panel, scheme of the relationship between the most accessible $\xi(\text{N}-\text{C}\alpha-\text{C}\beta-\text{C})$ dihedral angles and ${}^3J^{\text{isoD}}(\text{H}\alpha, \text{H}\beta)$ scalar couplings calculated according to a) Cung et al., b) De Marco et al. and c) Perez et al. parameters.

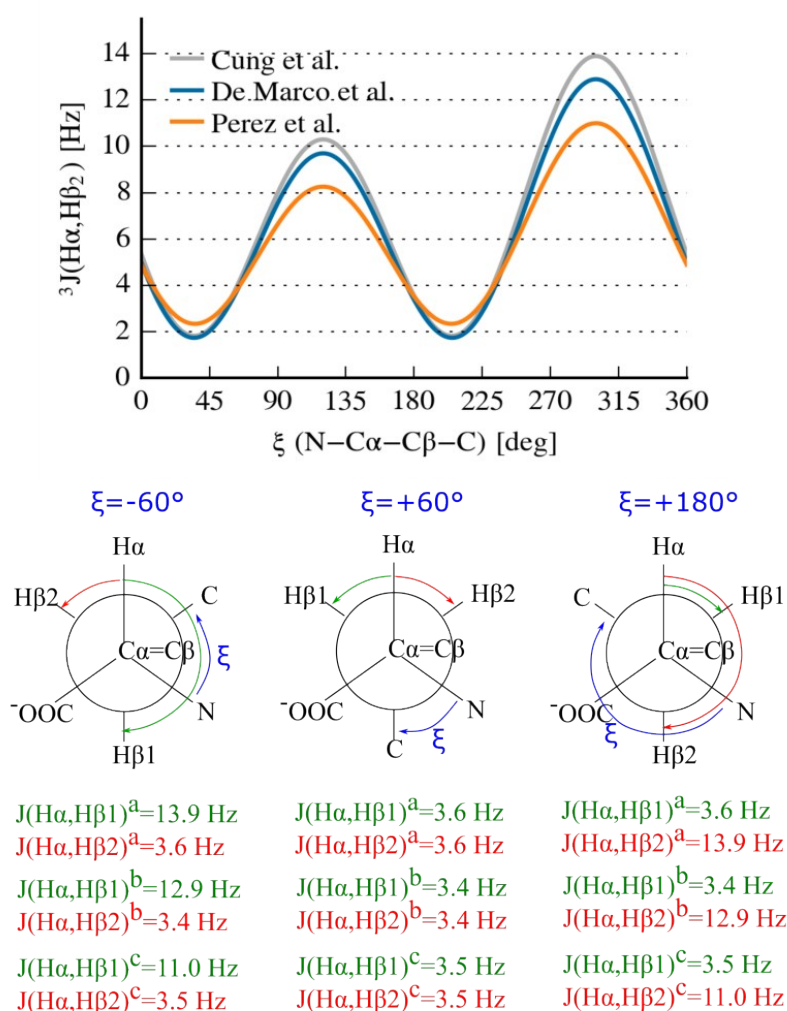


Figure S13. χ^2 values, estimating the ability of each force field to reproduce experimental $^3J(H\alpha, H\beta)$ scalar couplings, computed with the Karplus parameters developed by Cung et al. (light gray bars), De Marco et al. (blue bars) and Perez et al. (orange bars) are shown in the panel chart. The average χ^2 values and the error bar, representing the standard errors, have been computed adopting a Jack-Knife approach, in which the experimental data associated to one specific molecule have been sequentially excluded as described in Material and Methods. To avoid flattening of the data a zoom on the χ^2 range [0:10] is displayed in the lower panel.

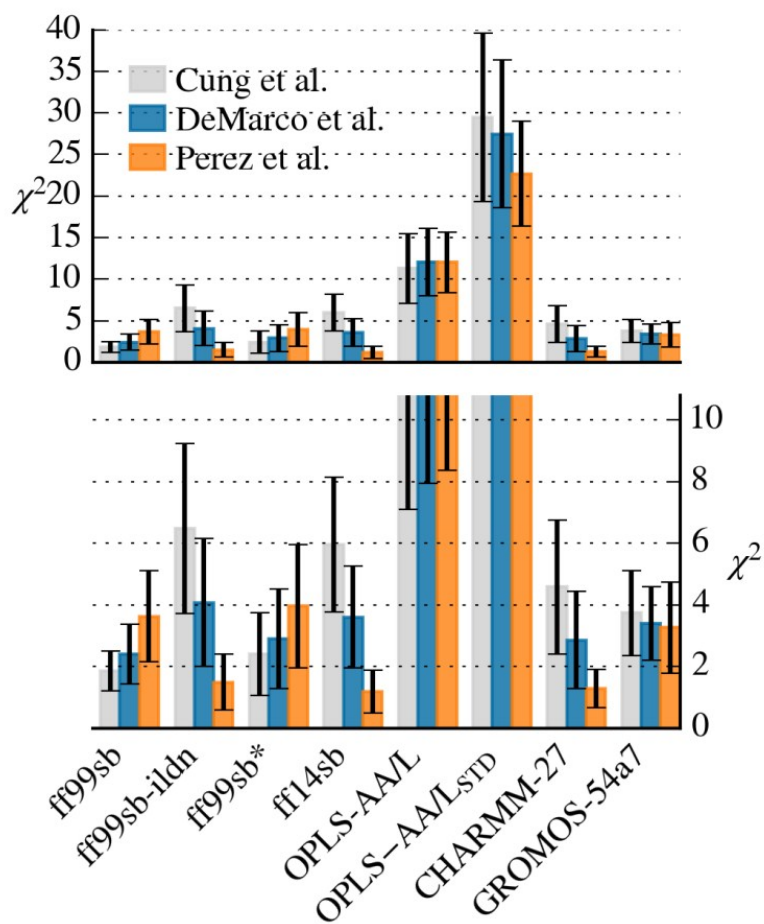


Figure S14. Comparison of the ${}^3J(\text{H}\alpha, \text{H}\beta)$ scalar couplings measured experimentally and back-calculated using the Karplus parameters developed by Cung et al. (upper panel) or Perez et al. (lower panel). The dark and light gray shadows indicate a deviation of ± 1 Hz and ± 2 Hz from experimental data, respectively. The r^2 value for linear regression of each force field is also reported.

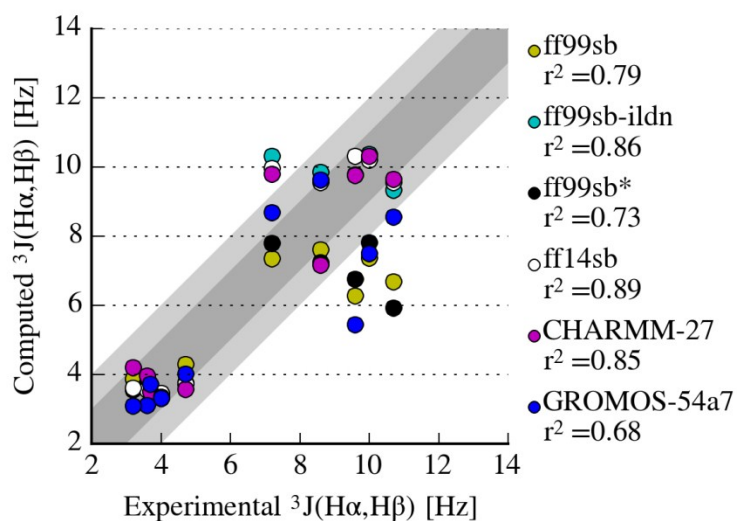
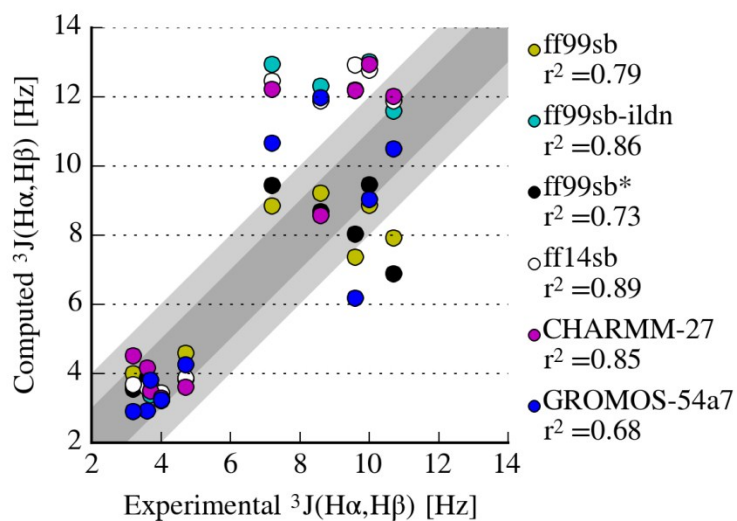


Figure S15. Correlation between $^3J(\text{HN}, \text{H}\alpha)$ scalar couplings computed with: i) AMBER ff99sb or ff99sb-ildn force fields, left panel; and ii) OPLS-AA/ L_{STD} or OPLS-AA/L force fields, right panel. All the $^3J(\text{HN}, \text{H}\alpha)$ scalar couplings have been computed using the DFT set of Karplus parameters.

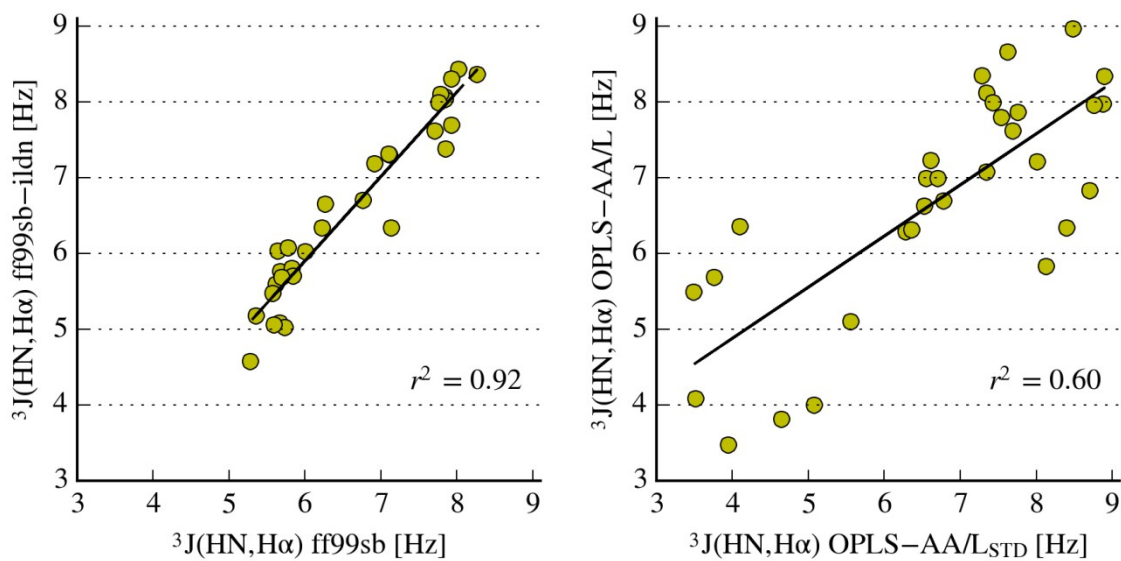
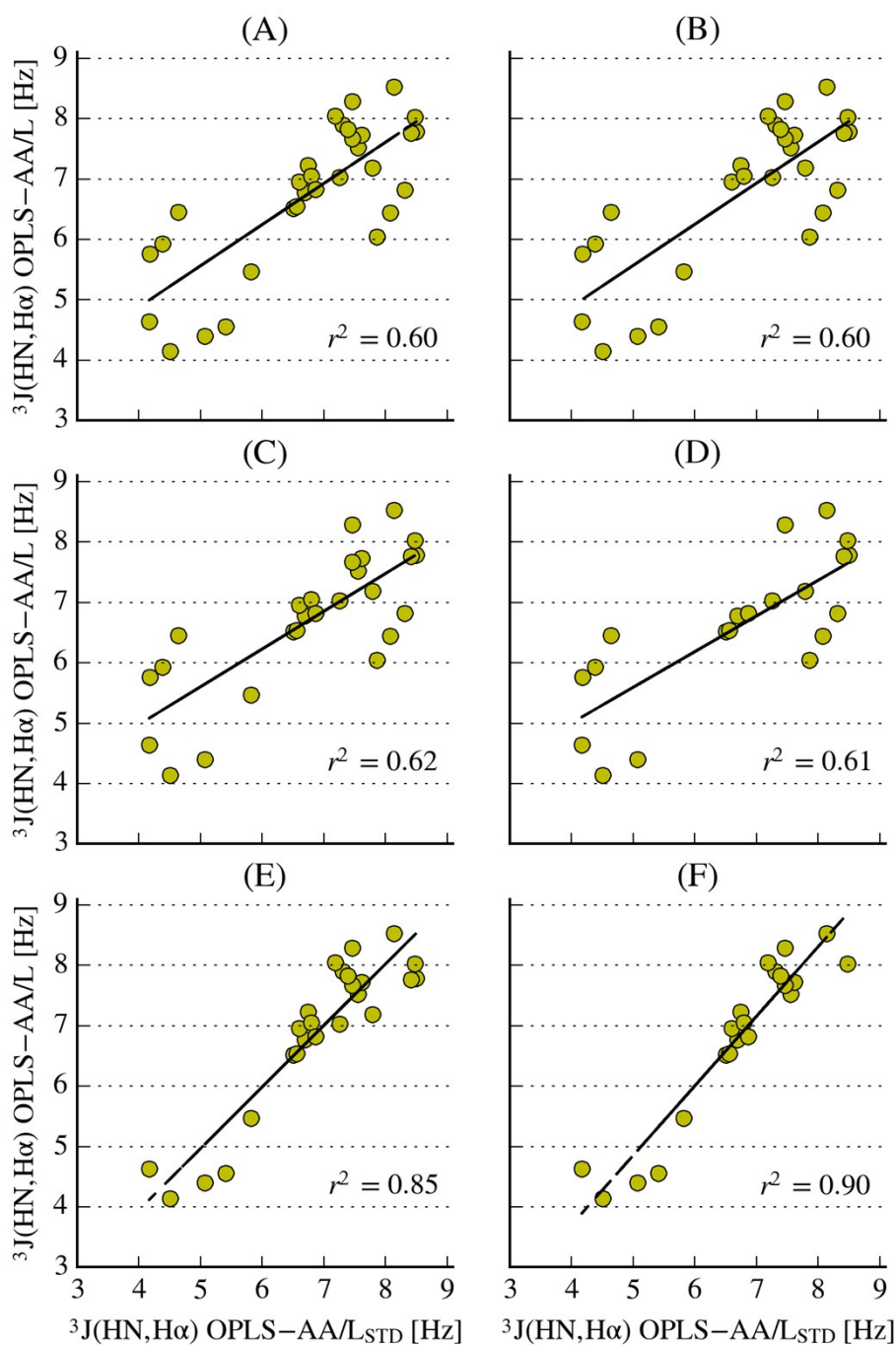


Figure S16. Correlation between $^3J(\text{HN},\text{H}\alpha)$ scalar couplings computed with the OPLS-AA/L_{STD} or OPLS-AA/L force fields, considering all the $^3J(\text{HN},\text{H}\alpha)$ (panel A) or excluding the subset of couplings related to: (B) isoAspartate, (C) the residue preceding isoAspartate, (D) the two residues preceding isoAspartate, (E) the residue following isoAspartate, (F) the two residues following isoAspartate. The $^3J(\text{HN},\text{H}\alpha)$ scalar couplings have been computed using both the ORIG (current page) and the DFT (next page) sets of Karplus parameters.



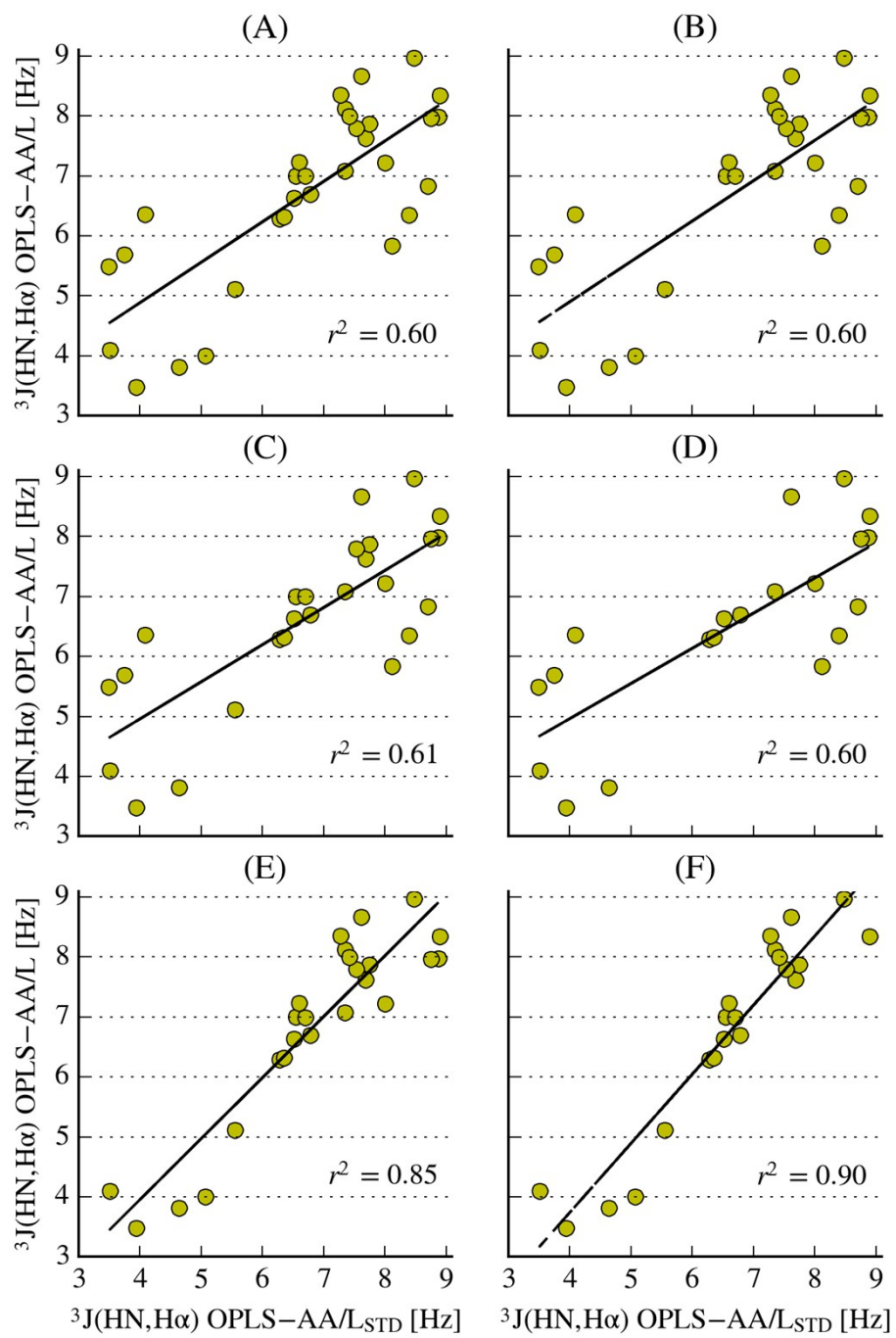
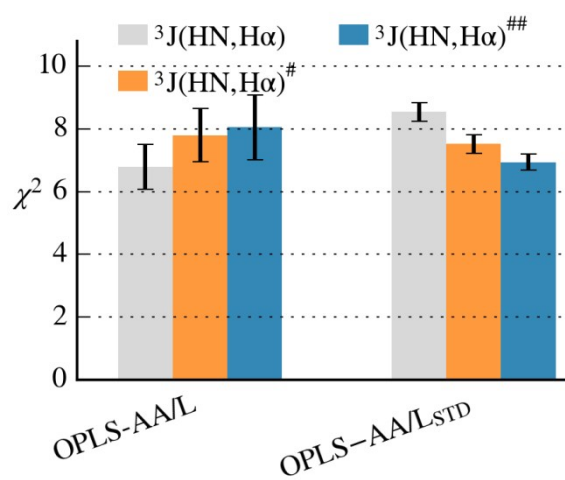


Figure S17. For the OPLS-AA/L and OPLS-AA/L_{STD} force fields, are reported the χ^2 values, estimating the ability to reproduce: i. all the experimental $^3J(\text{HN},\text{H}\alpha)$ couplings (gray bars), ii. all the $^3J(\text{HN},\text{H}\alpha)$ couplings except the ones of the residue following isoAspartate ($^3J(\text{HN},\text{H}\alpha)^\#$, orange bars), iii. all the $^3J(\text{HN},\text{H}\alpha)$ couplings except the ones of the two residues following isoAspartate ($^3J(\text{HN},\text{H}\alpha)^\#\#$, blue bars). The error bars represent the standard deviation of the χ^2 values obtained analyzing separately the first and the second halves of each simulation, as described in Material and Methods. All the $^3J(\text{HN},\text{H}\alpha)$ scalar couplings have been back-calculated using the DFT set of Karplus parameters.



REFERENCES

- 1 W. F. Vranken, W. Boucher, T. J. Stevens, R. H. Fogh, A. Pajon, M. Llinas, E. L. Ulrich, J. L. Markley, J. Ionides and E. D. Laue, *Proteins Struct. Funct. Genet.*, 2005, **59**, 687–696.
- 2 J. Graf, P. H. Nguyen, G. Stock and H. Schwalbe, *J. Am. Chem. Soc.*, 2007, **129**, 1179–1189.
- 3 D. A. Case, C. Scheurer and R. Bruschweiler, *J. Am. Chem. Soc.*, 2000, **122**, 10390–10397.
- 4 J. M. Schmidt, *J. Magn. Reson.*, 1997, **124**, 310–322.
- 5 J. R. Allison and W. F. Van Gunsteren, *ChemPhysChem*, 2009, **10**, 3213–3228.
- 6 A. Demarco, M. Llinás and K. Wüthrich, *Biopolymers*, 1978, **17**, 617–636.
- 7 A. Demarco, M. Llinás and K. Wüthrich, *Biopolymers*, 1978, **17**, 2727–2742.
- 8 C. Perez, F. Lohr, H. Ruterjans and J. M. Schmidt, *J. Am. Chem. Soc.*, 2001, **123**, 7081–7093.
- 9 Y. Shen and A. Bax, *J. Biomol. NMR*, 2010, **48**, 13–22.